

Evidence for a continuum limit in causal set dynamics

D. P. Rideout * and *R. D. Sorkin* †
Department of Physics, Syracuse University
Syracuse, NY, 13244-1130, U.S.A.

November 1, 2003

Abstract

We find evidence for a continuum limit of a particular causal set dynamics which depends on only a single “coupling constant” p and is easy to simulate on a computer. The model in question is a stochastic process that can also be interpreted as 1-dimensional directed percolation, or in terms of random graphs.

1 Introduction

In an earlier paper [1] we investigated a type of causal set dynamics that can be described as a (classically) stochastic process of growth or “accretion”. In a language natural to that dynamics, the passage of time consists in the continual birth of new elements of the causal set and the history of a sequence of such births can be represented as an upward path through a poset of all finite causal sets. We called such a stochastic process a *sequential growth dynamics* because the elements arise singly, rather than in pairs or larger multiplets.

A sequential description of this sort is advantageous in representing the future as developing out of the past, but on the other hand it could seem to rely on an external parameter time (the “time” in which the growth occurs), thereby violating the principle that physical time is encoded in the intrinsic order-relation of the causal set and nothing else. If physically real, such a parameter time would yield a distinguished labeling of the elements and thereby a notion of “absolute simultaneity”, in contradiction to the lessons of both special and general relativity. To avoid such a consequence, we postulated a principle of *discrete general covariance*, according to which no probability of the theory can depend on — and no physically meaningful question can refer to — the imputed order of births, except insofar as that order reflects the intrinsic precedence relation of the causal set itself.

To discrete general covariance, we added two other principles that we called *Bell causality* and *internal temporality*. The first is a discrete analog of the condition that no influence can propagate faster than light, and the second simply requires that no element be born to the past of any existing element.¹ These principles led us almost uniquely to a family of dynamical laws (stochastic processes) parameterized by a countable sequence of coupling constants q_n . In addition to this generic family, there are some exceptional families of solutions, but we conjecture that they are all singular limits of the generic family. We have checked in particular that “ordinary percolation” (see section 2) is such a limit.²

*rideout@physics.syr.edu

†sorkin@physics.syr.edu

¹This last condition guarantees that the “parameter time” of our stochastic process *is compatible with* physical temporality, as recorded in the order relation \prec that gives the causal set its structure. In a broader sense, general covariance itself is also an aspect of internal temporality, since it guarantees that the parameter time *adds nothing to* the relation \prec .

²In the notation of [1], it is the $A \rightarrow \infty$ limit of the dynamics given by $t_0 = 1$, $t_n = At^n$, $n = 1, 2, 3, \dots$

Now among these dynamical laws, the one resulting from the choice $q_n = q^n$ is one of the easiest to work with, both conceptually and for purposes of computer simulation. Defined by a single real parameter $q \in [0, 1]$, it is described in more detail in Section 2 below. In [1], we referred to it as *transitive percolation* because it can be interpreted in terms of a random “turning on” of nonlocal bonds (with probability $p = 1 - q$) in a one-dimensional lattice. Another thing making it an attractive special case to work with is the availability in the mathematics literature of a number of results governing the asymptotic behavior of posets generated in this manner [2, 3].

Aside from its convenience, this percolation dynamics, as we will call it, possesses other distinguishing features, including an underlying time-reversal invariance and a special relevance to causal set cosmology, as we describe briefly below. In this paper, we search for evidence of a continuum limit of percolation dynamics.

One might question whether a continuum limit is even desirable in a fundamentally discrete theory, but a continuum *approximation* in a suitable regime is certainly necessary if the theory is to reproduce known physics. Given this, it seems only a small step to a rigorous continuum limit, and conversely, the existence of such a limit would encourage the belief that the theory is capable of yielding continuum physics with sufficient accuracy.

Perhaps an analogy with kinetic theory can guide us here. In quantum gravity, the discreteness scale is set, presumably, by the Planck length $l = (\kappa\hbar)^{1/2}$ (where $\kappa = 8\pi G$), whose vanishing therefore signals a continuum limit. In kinetic theory, the discreteness scales are set by the mean free path λ and the mean free time τ , both of which must go to zero for a description by partial differential equations to become exact. Corresponding to these two independent length and time scales are two “coupling constants”: the diffusion constant D and the speed of sound c_{sound} . Just as the value of the gravitational coupling constant $G\hbar$ reflects (presumably) the magnitude of the fundamental spacetime discreteness scale, so the values of D and c_{sound} reflect the magnitudes of the microscopic parameters λ and τ according to the relations

$$D \sim \frac{\lambda^2}{\tau}, \quad c_{\text{sound}} \sim \frac{\lambda}{\tau}$$

or conversely

$$\lambda \sim \frac{D}{c_{\text{sound}}}, \quad \tau \sim \frac{D}{c_{\text{sound}}^2}.$$

In a continuum limit of kinetic theory, therefore, we must have either $D \rightarrow 0$ or $c_{\text{sound}} \rightarrow \infty$. In the former case, we can hold c_{sound} fixed, but we get a purely mechanical macroscopic world, without diffusion or viscosity. In the latter case, we can hold D fixed, but we get a “purely diffusive” world with mechanical forces propagating at infinite speed. In each case we get a well defined — but defective — continuum physics, lacking some features of the true, atomistic world.

If we can trust this analogy, then something very similar must hold in quantum gravity. To send l to zero, we must make either G or \hbar vanish. In the former case, we would expect to obtain a quantum world with the metric decoupled from non-gravitational matter; that is, we would expect to get a theory of quantum field theory in a purely classical background spacetime solving the source-free Einstein equations. In the latter case, we would expect to obtain classical general relativity. Thus, there might be two distinct continuum limits of quantum gravity, each physically defective in its own way, but nonetheless well defined.

For our purposes in this paper, the important point is that, although we would not expect quantum gravity to exist as a continuum theory, it could have limits which do, and one of these limits might be classical general relativity. It is thus sensible to inquire whether one of the classical causal set dynamics we have defined describes classical spacetimes. In the following, we make a beginning on this question by asking whether the special case of “percolated causal sets”, as we will call them, admits a continuum limit at all.

Of course, the physical content of any continuum limit we might find will depend on what we hold fixed in passing to the limit, and this in turn is intimately linked to how we choose the coarse-graining

procedure that defines the effective macroscopic theory whose existence the continuum limit signifies. Obviously, we will want to send $N \rightarrow \infty$ for any continuum limit, but it is less evident how we should coarse-grain and what coarse grained parameters we want to hold fixed in taking the limit. Indeed, the appropriate choices will depend on whether the macroscopic spacetime region we have in mind is, to take some naturally arising examples, (i) a fixed bounded portion of Minkowski space of some dimension, or (ii) an entire cycle of a Friedmann universe from initial expansion to final recollapse, or (iii) an N -dependent portion of an unbounded spacetime M that expands to encompass all of M as $N \rightarrow \infty$. In the sequel, we will have in mind primarily the first of the three examples just listed. Without attempting an definitive analysis of the coarse-graining question, we will simply adopt the simplest definitions that seem to us to be suited to this example. More specifically, we will coarse-grain by randomly selecting a sub-causal-set of a fixed number of elements, and we will choose to hold fixed some convenient invariants of that sub-causal-set, one of which can be interpreted³ as the dimension of the spacetime region it constitutes. As we will see, the resulting scheme has much in common with the kind of coarse-graining that goes into the definition of renormalizability in quantum field theory. For this reason, we believe it can serve also as an instructive “laboratory” in which this concept, and related concepts like “running coupling constant” and “non-trivial fixed point”, can be considered from a fresh perspective.

In the remaining sections of this paper we: define transitive percolation dynamics more precisely; specify the coarse-graining procedure we have used; report on the simulations we have run looking for a continuum limit in the sense thereby defined; and offer some concluding comments.

1.1 Definitions used in the sequel

Causal set theory postulates that spacetime, at its most fundamental level, is discrete, and that its macroscopic geometrical properties reflect a deep structure which is purely order theoretic in nature. This deep structure is taken to be a partial order and called a causal set (or “causet” for short). For an introduction to causal set theory, see [4, 5, 6, 7]. In this section, we merely recall some definitions which we will be using in the sequel.

A (*partial*) *order* or *poset* is a set S endowed with a relation \prec which is:

$$\begin{array}{ll} \text{transitive} & \forall x, y, z \in S \quad x \prec y \text{ and } y \prec z \Rightarrow x \prec z \\ \text{acyclic} & \forall x, y \in S \quad x \prec y \Rightarrow y \not\prec x \\ \text{irreflexive} & \forall x \in S \quad x \not\prec x \end{array}$$

(Irreflexivity is merely a convention; with it, acyclicity is actually redundant.) For example, the events of Minkowski space (in any dimension) form a poset whose order relation is the usual causal order. In an order S , the *interval* $\text{int}(x, y)$ is defined to be

$$\text{int}(x, y) = \{z \in S \mid x \prec z \prec y\} .$$

An order is said to be *locally finite* if all its intervals are finite (have finite cardinality). A *causal set* is a locally finite order.

It will be helpful to have names for some small causal sets. Figure 1.1 provides such names for the causal sets with three or fewer elements.

2 The dynamics of transitive percolation

Regarded as a sequential growth dynamics of the sort derived in [1], transitive percolation is described by one free parameter q such that $q_n = q^n$. This is equivalent (at stage N of the growth process) to using the following “percolation” algorithm to generate a random causet.

³This interpretation is strictly correct only if the causal set forms an *interval* or “Alexandrov neighborhood” within the spacetime.

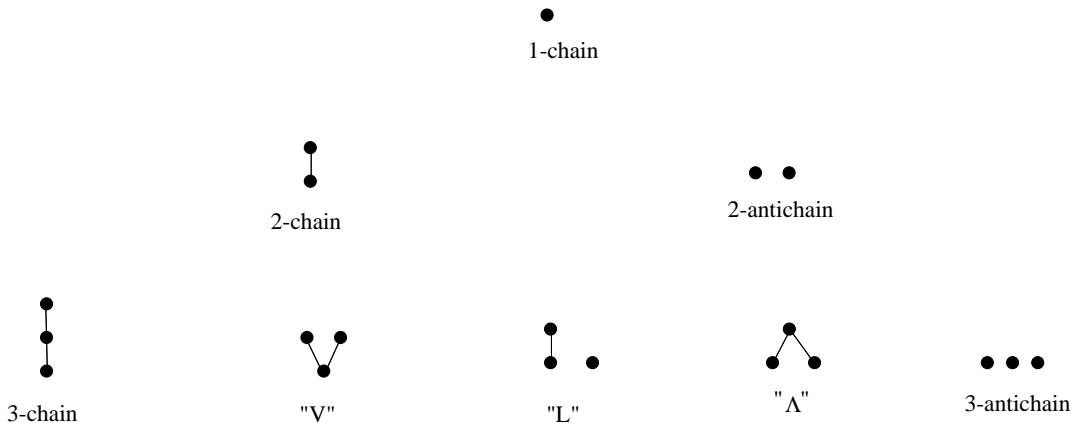


Figure 1: Names for small causets

1. Start with N elements labeled $0, 1, 2, \dots, N - 1$.
2. With a fixed probability p ($= 1 - q$), introduce a relation $i \prec j$ between every pair of elements labeled i and j , where $i \in \{0 \cdots N - 2\}$ and $j \in \{i + 1 \cdots N - 1\}$.
3. Form the transitive closure of these relations (e.g. if $2 \prec 5$ and $5 \prec 8$ then enforce that $2 \prec 8$.)

Given the simplicity of this dynamical model, both conceptually and from an algorithmic standpoint, it offers a “stepping stone” allowing us to look into some general features of causal set dynamics. (The name “percolation” comes from thinking of a relation $i \prec j$ as a “bond” or “channel” between i and j .)

There exists another model which is very similar to transitive percolation, called “originary transitive percolation”. The rule for randomly generating a causet is the same as for transitive percolation, except that each new element is required to be related to at least one existing element. Algorithmically, we generate potential elements one by one, exactly as for plain percolation, but discard any such element which would be unrelated to all previous elements. Causets formed with this dynamics always have a single minimal element, an “origin”.

Recent work by Dou [8] suggests that originary percolation might have an important role to play in cosmology. Notice first that, if a given cosmological “cycle” ends with the causet collapsing down to a single element, then the ensuing re-expansion is necessarily given by an originary causet. Now, in the limited context of percolation dynamics, Alon *et al.* have proved rigorously [3] that such cosmological “bounces” (which they call *posts*) occur with probability 1 (if $p > 0$), from which it follows that there are infinitely many cosmological cycles, each cycle but the first having the dynamics of originary percolation. For more general choices of the dynamical parameters q_n of [1], posts can again occur, but now the q_n take on new effective values in each cycle, related to the old ones by the action of a sort of “cosmological renormalization group”; and Dou [8] has found evidence that originary percolation is a “stable fixed point” of this action, meaning that the universe would tend to evolve toward this behavior, no matter what dynamics it began with.

It would thus be of interest to investigate the continuum limit of originary percolation as well as plain percolation. In the present paper, however, we limit ourselves to the latter type, which we believe is more appropriate (albeit not fully appropriate for reasons discussed in the conclusion) in the context of spacetime regions of sub-cosmological scale.

3 The critical point at $p = 0$, $N = \infty$

In the previous section we have introduced a model of random causets, which depends on two parameters, $p \in [0, 1]$ and $N \in \mathbb{N}$. For a given p , the model defines a probability distribution on the set of N -element causets.⁴ For $p = 0$, the only causet with nonzero probability, obviously, is the N -antichain. Now let $p > 0$. With a little thought, one can convince oneself that for $N \rightarrow \infty$, the causet will look very much like a chain. Indeed it has been proved [9] (see also [10]) that, as $N \rightarrow \infty$ with p fixed at some (arbitrarily small) positive number, $r \rightarrow 1$ in probability, where

$$r \equiv \frac{R}{N(N-1)/2} = \frac{R}{\binom{N}{2}},$$

R being the number of relations in the causet, i.e. the number of pairs of causet elements x, y such that $x \prec y$ or $y \prec x$. Note that the N -chain has the greatest possible number $\binom{N}{2}$ of relations, so $r \rightarrow 1$ gives a precise meaning to “looking like a chain”. We call r the *ordering fraction* of the causal set, following [11].

We see that for $N \rightarrow \infty$, there is a change in the qualitative nature of the causet as p varies away from zero, and the point $p = 0$, $N = \infty$ (or $p = 1/N = 0$) is in this sense a critical point of the model. It is the behavior of the model near this critical point which will concern us in this paper.

4 Coarse graining

An advantageous feature of causal sets is that there exists for them a simple yet precise notion of coarse graining. A coarse grained approximation to a causet C can be formed by selecting a sub-causet C' at random, with equal selection probability for each element, and with the causal order of C' inherited directly from that of C (i.e. $x \prec y$ in C' if and only if $x \prec y$ in C .)

For example, let us start with the 20 element causet C shown in Figure 2. (which was percolated using $p = 0.25$), and successively coarse grain it down to causets of 10, 5 and 3 elements. We see that, at the largest scale shown (i.e. the smallest number of remaining elements), C has coarse-grained in this instance to the 3-element “V” causet. Of course, coarse graining itself is a random process, so from a single causet of N elements, it gives us in general, not another single causet, but a probability distribution on the causets of $m < N$ elements.

A noteworthy feature of this definition of coarse graining, which in some ways is similar to what is often called “decimation” in the context of spin systems, is the *random* selection of a subset. In the absence of any background lattice structure to refer to, no other possibility for selecting a sub-causet is evident. Random selection is also recommended strongly by considerations of Lorentz invariance [12]. The fact that a coarse grained causet is automatically another causet will make it easy for us to formulate precise notions of continuum limit, running of the coupling constant p , etc. In this respect, we believe that this model combines precision with novelty in such a manner as to furnish an instructive illustration of concepts related to renormalizability, independently of its application to quantum gravity. We remark in this connection, that transitive percolation is readily embedded in a “two-temperature” statistical mechanics model, and as such, happens also to be exactly soluble in the sense that the partition function can be computed exactly [13, 14].

⁴Strictly speaking this distribution has gauge-invariant meaning only in the limit $N \rightarrow \infty$ (p fixed); for it is only insofar as the growth process “runs to completion” that generally covariant questions can be asked. Notice that this limit is inherent in causal set dynamics itself, and has nothing to do with the continuum limit we are concerned with herein, which sends p to zero as $N \rightarrow \infty$.

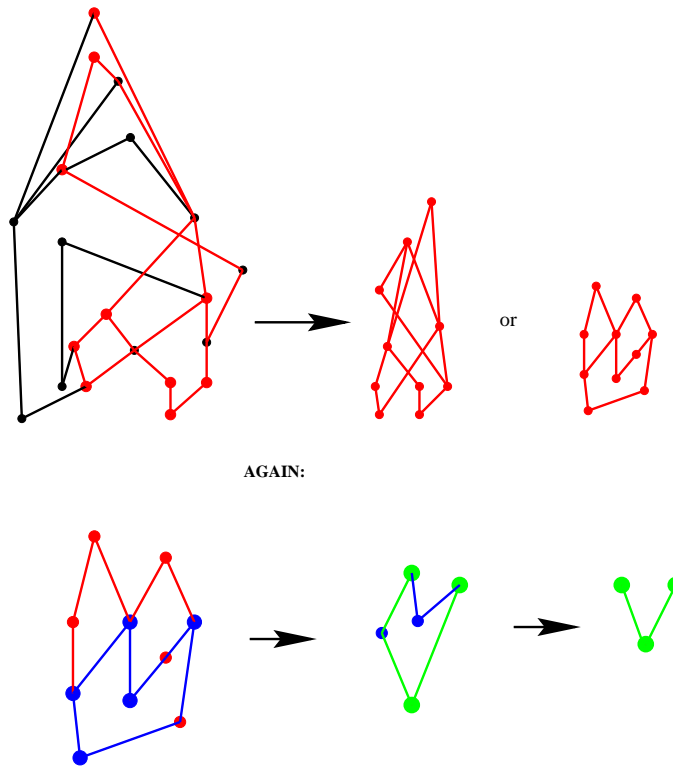


Figure 2: Three successive coarse grainings of a 20-element causet

5 The large scale effective theory

In section 2 we described a “microscopic” dynamics for causal sets (that of transitive percolation) and in section 4 we defined a precise notion of coarse graining (that of random selection of a sub-causal-set). On this basis, we can produce an effective “macroscopic” dynamics by imagining that a causet C is first percolated with N elements and then coarse-grained down to $m < N$ elements. This two-step process constitutes an effective random procedure for generating m element causets depending (in addition to m) on the parameters N and p . In causal set theory, number of elements corresponds to spacetime volume, so we can interpret N/m as the factor by which the “observation scale” has been increased by the coarse graining. If, then, V_0 is the macroscopic volume of the spacetime region constituted by our causet, and if we take V_0 to be fixed as $N \rightarrow \infty$, then our procedure for generating causets of m elements provides the effective dynamics at volume-scale V_0/m (i.e. length scale $(V_0/m)^{1/d}$ for a spacetime of dimension d).

What does it mean for our effective theory to have a continuum limit in this context? Our stochastic microscopic dynamics gives, for each choice of p , a probability distribution on the set of causal sets C with N elements, and by choosing m , we determine at which scale we wish to examine the corresponding effective theory. This effective theory is itself just a probability distribution f_m on the set of m -element causets, and so our dynamics will have a well defined continuum limit if there exists, as $N \rightarrow \infty$, a trajectory $p = p(N)$ along which the corresponding probability distributions f_m on coarse grained causets approach fixed limiting distributions f_m^∞ for all m . The limiting theory in this sense is then a sequence of effective theories, one for each m , all fitting together consistently. (Thanks to the associative (semi-group) character of our coarse-graining procedure, the existence of a limiting distribution for any given m implies its existence for all smaller m . Thus it suffices that a limiting distribution f_m exist for m arbitrarily large.) In general there will exist not just a single such trajectory $p = p(N)$, but a one-parameter family of them (corresponding to the one real parameter p that characterizes the microscopic dynamics at any fixed N),

and one may wonder whether all the trajectories will take on the same asymptotic form as they approach the critical point $p = 1/N = 0$.

Consider first the simplest nontrivial case, $m = 2$. Since there are only two causal sets of size two, the 2-chain and the 2-antichain, the distribution f_2 that gives the “large scale physics” in this case is described by a single number which we can take to be $f_2(\mathbf{!})$, the probability of obtaining a 2-chain rather than a 2-antichain. (The other probability, $f_2(\bullet\bullet)$, is of course not independent, since classical probabilities must add up to unity.)

Interestingly enough, the number $f_2(\mathbf{!})$ has a direct physical interpretation in terms of the Myrheim-Meyer dimension of the fine-grained causet C . Indeed, it is easy to see that $f_2(\mathbf{!})$ is nothing but the expectation value of what was called above the “ordering fraction” of C . But the ordering fraction, in turn, determines the Myrheim-Meyer dimension d that indicates the dimension of the Minkowski spacetime \mathbb{M}^d (if any) in which C would embed faithfully as an interval [15, 11]. Thus, by coarse graining down to two elements, we are effectively measuring a certain kind of spacetime dimensionality of C . In practice, we would not expect C to embed faithfully without some degree of coarse-graining, but the original r would still provide a good dimension estimate since it is, on average, coarse-graining invariant.

As we begin to consider coarse-graining to sizes $m > 2$, the degree of complication grows rapidly, simply because the number of partial orders defined on m elements grows rapidly with m . For $m = 3$ there are five possible causal sets: $\mathbf{!}$, \mathbf{V} , $\mathbf{!..}$, $\mathbf{\wedge}$, and $\mathbf{...}$. Thus the effective dynamics at this “scale” is given by five probabilities (so four free parameters). For $m = 4$ there are sixteen probabilities, for $m = 5$ there are sixty three, and for $m = 6, 7$ and 8 , the number of probabilities is respectively 318, 2045 and 16999.

6 Evidence from simulations

In this section, we report on some computer simulations that address directly the question whether transitive percolation possesses a continuum limit in the sense defined above. In a subsequent paper, we will report on simulations addressing the subsidiary question of a possible scaling behavior in the continuum limit.

In order that a continuum limit exist, it must be possible to choose a trajectory for p as a function of N so that the resulting coarse-grained probability distributions, f_1, f_2, f_3, \dots , have well defined limits as $N \rightarrow \infty$. To study this question numerically, one can simulate transitive percolation using the algorithm described in Section 2, while choosing p so as to hold constant (say) the $m = 2$ distribution f_2 (f_1 being trivial). Because of the way transitive percolation is defined, it is intuitively obvious that p can be chosen to achieve this, and that in doing so, one leaves p with no further freedom. The decisive question then is whether, along the trajectory thereby defined, the higher distribution functions, f_3, f_4 , etc. all approach nontrivial limits.

As we have already mentioned, holding f_2 fixed is the same thing as holding fixed the expectation value $\langle r \rangle$ of ordering fraction $r = R/\binom{N}{2}$. To see in more detail why this is so, consider the coarse-graining that takes us from the original causet C_N of N elements to a causet C_2 of two elements. Since coarse-graining is just random selection, the probability $f_2(\mathbf{!})$ that C_2 turns out to be a 2-chain is just the probability that two elements of C_N selected at random form a 2-chain rather than a 2-antichain. In other words, it is just the probability that two elements of C_N selected at random are causally related. Plainly, this is the same as the *fraction* of pairs of elements of C_N such that the two members of the pair form a relation $x \prec y$ or $y \prec x$. Therefore, the ordering fraction r equals the probability of getting a 2-chain when coarse graining C_N down to two elements; and $f_2(\mathbf{!}) = \langle r \rangle$, as claimed.

This reasoning illustrates, in fact, how one can in principle determine any one of the distributions f_m by answering the question, “What is the probability of getting this particular m -element causet from this particular N -element causet if you coarse grain down to m elements?” To compute the answer to such

a question starting with any given causet C_N , one examines every possible combination of m elements, counts the number of times that the combination forms the particular causet being looked for, and divides the total by $\binom{N}{m}$. The ensemble mean of the resulting *abundance*, as we will refer to it, is then $f_m(\xi)$, where ξ is the causet being looked for. In practice, of course, we would normally use a more efficient counting algorithm than simply examining individually all $\binom{N}{m}$ subsets of C_N .

6.1 Histograms of 2-chain and 4-chain abundances

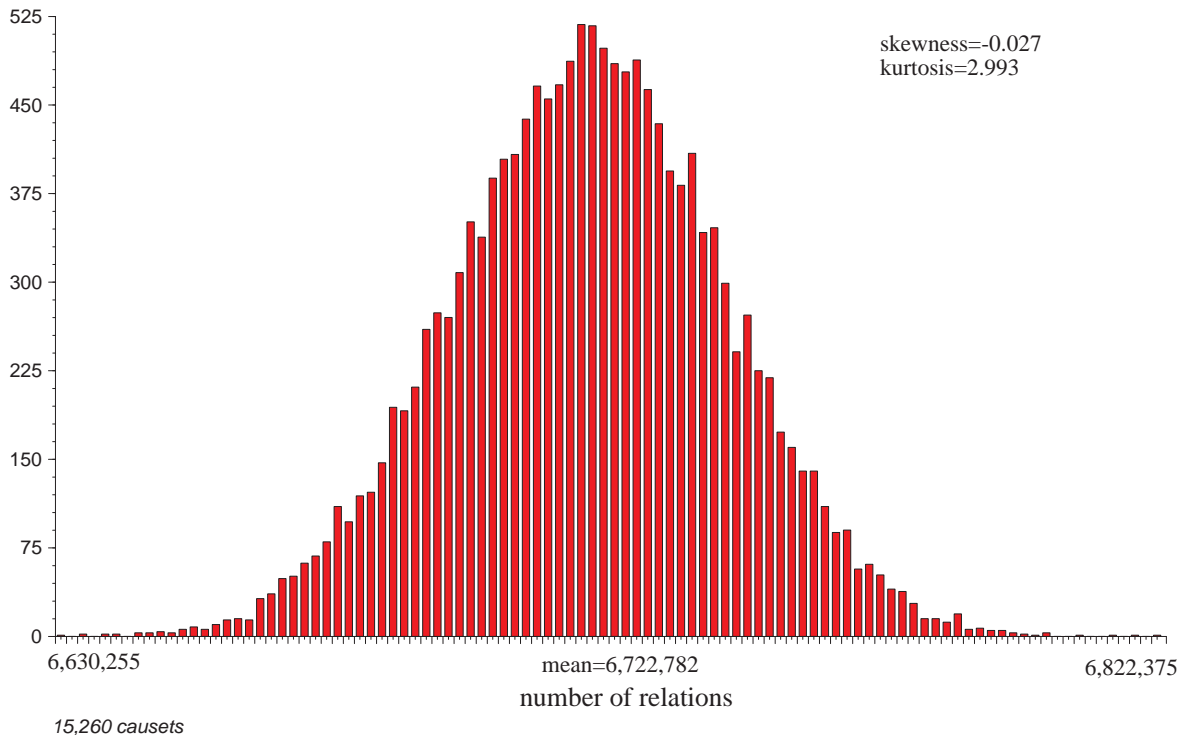


Figure 3: Distribution of number of relations for $N = 4096$, $p = 0.01155$

As explained in the previous subsection, the main computational problem, once the random causet has been generated, is determining the number of subcausets of different sizes and types. To get a feel for how some of the resulting “abundances” are distributed, we start by presenting a couple of histograms. Figure 6.1 shows the number R of relations obtained from a simulation in which 15,260 causal sets were generated by transitive percolation with $p = 0.01155$, $N = 4096$. Visually, the distribution is Gaussian, in agreement with the fact that its “kurtosis”

$$\frac{\overline{(x - \bar{x})^4}}{\overline{(x - \bar{x})^2}^2}$$

of 2.993 is very nearly equal to its Gaussian value of 3 (the over-bar denotes sample mean). In these simulations, p was chosen so that the number of 3-chains was equal on average to half the total number possible, i.e. the “abundance of 3-chains”, $(\text{number of 3-chains})/\binom{N}{3}$, was equal to $1/2$ on average. The picture is qualitatively identical if one counts 4-chains rather than 2-chains, as exhibited in Fig. 4.

(One may wonder whether it was to be expected that these distributions would appear to be so normal. If the variable in question, here the number of 2-chains R or the number of 4-chains (C_4 , say),

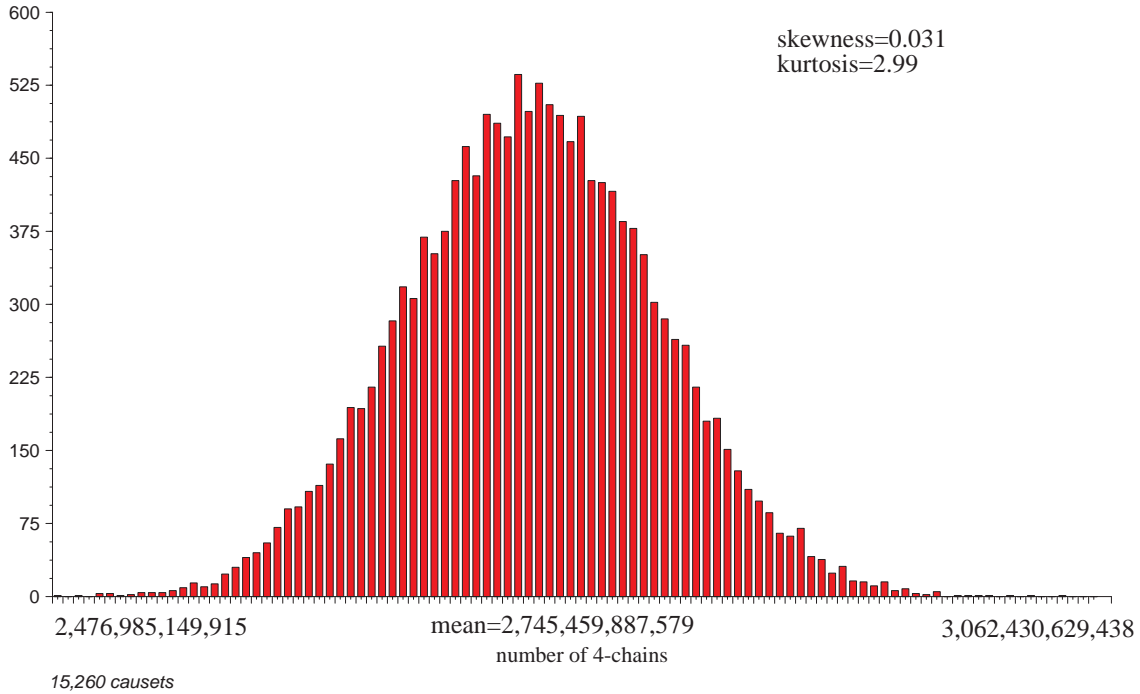


Figure 4: Distribution of number of 4-chains for $N = 4096$, $p = 0.01155$

can be expressed as a sum of independent random variables, then the central limit theorem provides an explanation. So consider the variables x_{ij} which are 1 if $i \prec j$ and zero otherwise. Then R is easily expressed as a sum of these variables:

$$R = \sum_{i < j} x_{ij}$$

However, the x_{ij} are not independent, due to transitivity. Apparently, this dependence is not large enough to interfere much with the normality of their sum. The number of 4-chains C_4 can be expressed in a similar manner

$$C_4 = \sum_{i < j < k < l} x_{ij} x_{jk} x_{kl}.$$

and similar remarks apply.)

Let us mention that for values of p sufficiently close to 0 or 1, these distributions will appear skew. This occurs simply because the numbers under consideration (e.g. the number of m -chains) are bounded between zero and $\binom{N}{m}$ and must deviate from normality if their mean gets too close to a boundary relative to the size of their standard deviation. Whenever we draw an error bar in the following, we will ignore any deviation from normality in the corresponding distribution.

Notice incidentally that the total number of 4-chains possible is $\binom{4096}{4} = 11,710,951,848,960$. Consequently, the mean 4-chain abundance⁵ in our simulation is only $\frac{2,745,459,887,579}{11,710,951,848,960} = 0.234$, a considerably smaller value than the 2-chain abundance of $r = \frac{6,722,782}{\binom{4096}{2}} = 0.802$. This was to be expected, considering that the 2-chain is one of only two possible causets of its size, while the 4-chain is one out 16 possibilities.

⁵From this point on we will usually write simply “abundance”, in place of “mean abundance”, assuming the average is obvious from context.

(Notice also that 4-chains are necessarily less probable than 2-chains, because every coarse-graining of a 4-chain is a 2-chain, whereas the 2-chain can come from every 4-element causet save the 4-antichain.)

6.2 Trajectories of p versus N

The question we are exploring is whether there exist, for $N \rightarrow \infty$, trajectories $p = p(N)$ along which the mean abundances of all finite causets tend to definite limits. To seek such trajectories numerically, we will select some finite “reference causet” and determine, for a range of N , those values of p which maintain its abundance at some target value. If a continuum limit does exist, then it should not matter in the end which causet we select as our reference, since any other choice (together with a matching choice of target abundance) should produce the same trajectory asymptotically. We would also anticipate that all the trajectories would behave similarly for large N , and that, in particular, either all would lead to continuum limits or all would not. In principle it could happen that only a certain subset led to continuum limits, but we know of no reason to expect such an eventuality. In the simulations reported here, we have chosen as our reference causets the 2-, 3- and 5-chains. We have computed six trajectories, holding the 2-chain abundance fixed at $1/2$, $1/3$, and $1/10$, the 3-chain abundance fixed at $1/2$ and $.0814837$, and the 5-chain abundance fixed at $1/2$. For N , we have used as large a range as our computers would allow.

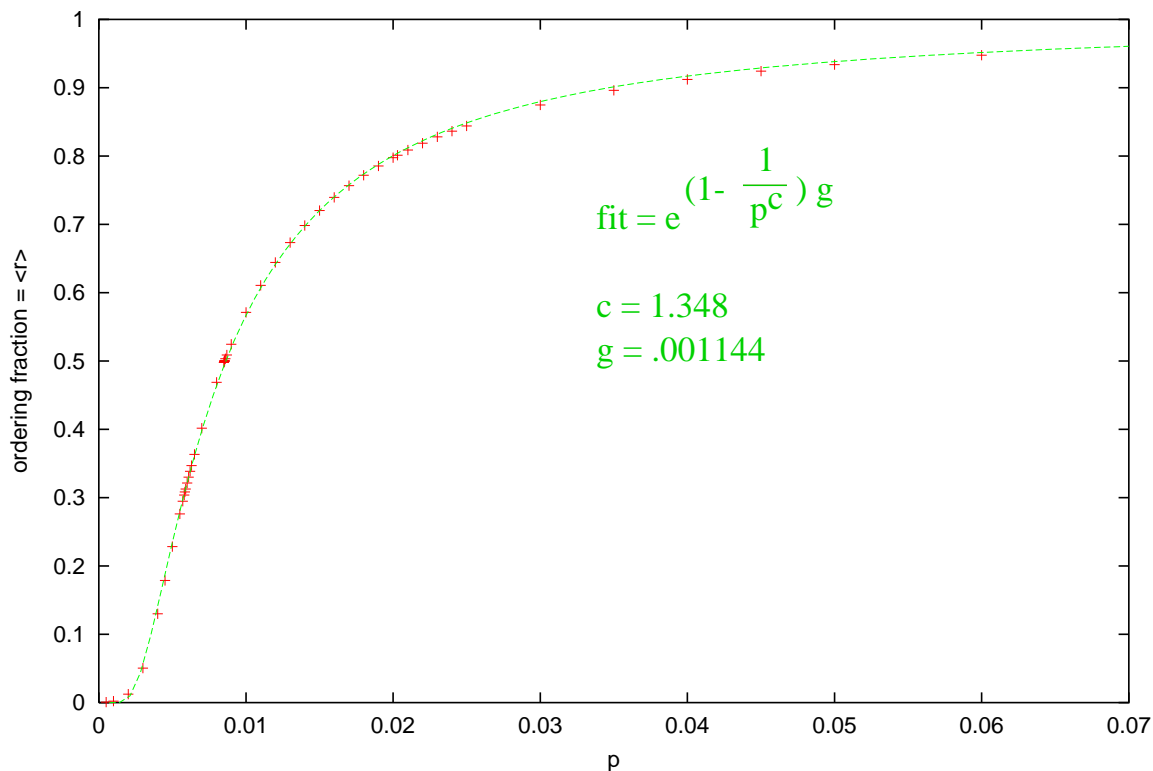


Figure 5: Ordering fractions as a function of p for $N = 2048$

Before discussing the trajectories as such, let us have a look at how the mean 2-chain abundance $\langle r \rangle$ (i.e. the mean ordering fraction) varies with p for a fixed N of 2048, as exhibited in Figure 5. (Vertical error bars are displayed in the figure but are so small that they just look like horizontal lines. The plotted points were obtained from an exact expression for the ensemble average $\langle r \rangle$, so the errors come only from floating point roundoff. The fitting function used in Figure 5 will be discussed in a subsequent paper [14], where we examine scaling behavior; see also [2].) As one can see, $\langle r \rangle$ starts at 0 for $p = 0$,

risers rapidly to near 1 and then asymptotes to 1 at $p = 1$ (not shown). Of course, it was evident a priori that $\langle r \rangle$ would increase monotonically from 0 to 1 as p varied between these same two values, but it is perhaps noteworthy that its graph betrays no sign of discontinuity or non-analyticity (no sign of a “phase transition”). To this extent, it strengthens the expectation that the trajectories we find will all share the same qualitative behavior as $N \rightarrow \infty$.

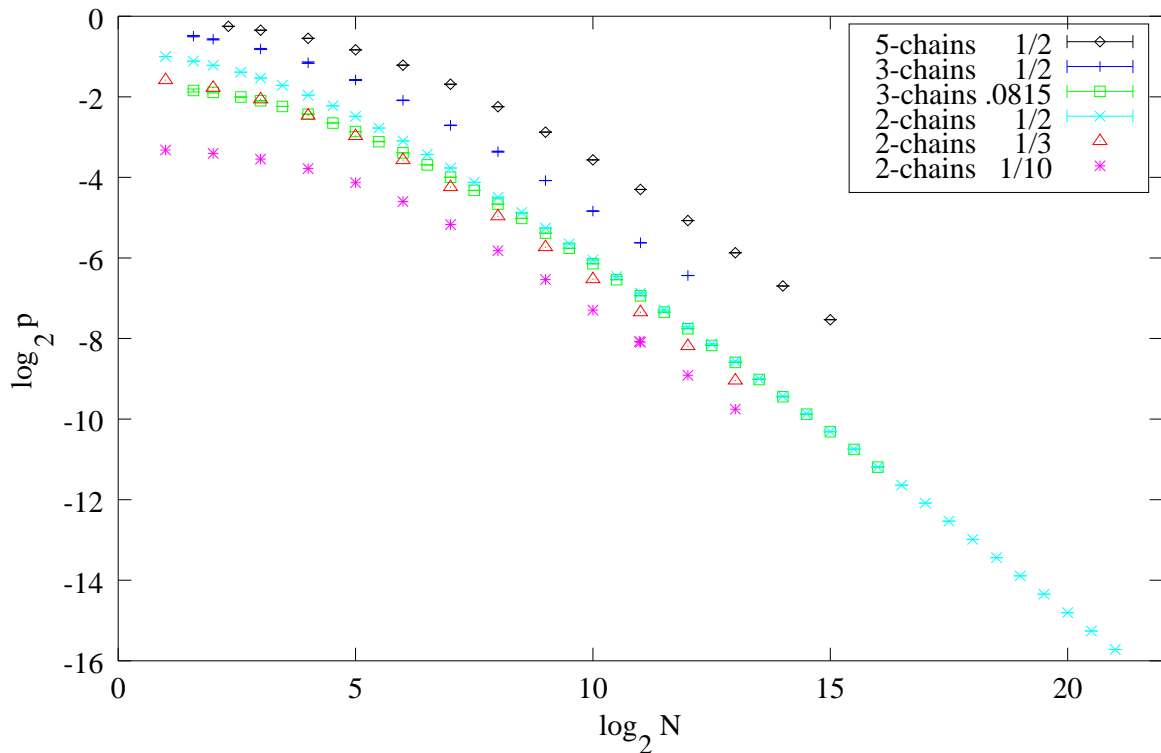


Figure 6: Flow of the “coupling constant” p as $N \rightarrow \infty$ (six trajectories)

The six trajectories we have simulated are depicted in Fig. 6.⁶ A higher abundance of m -chains for fixed m leads to a trajectory with higher p . Also note that, as observed above, the longer chains require larger values of p to attain the same mean abundance, hence a choice of mean abundance = $1/2$ corresponds in each case to a different trajectory. The trajectories with $\langle r \rangle$ held to lower values are “higher dimensional” in the sense that $\langle r \rangle = 1/2$ corresponds to a Myrheim-Meyer dimension of 2, while $\langle r \rangle = 1/10$ corresponds to a Myrheim-Meyer dimension of 4. Observe that the plots give the impression of becoming straight lines with a common slope at large N . This tends to corroborate the expectation that they will exhibit some form of scaling with a common exponent, a behavior reminiscent of that found with continuum limits in many other contexts. This is further suggested by the fact that two distinct trajectories ($f_2(\mathbf{1}) = 1/2$ and $f_3(\mathbf{1}) = .0814837$), obtained by holding different abundances fixed, seem to converge for large N .

By taking the abscissa to be $1/N$ rather than $\log_2 N$, we can bring the critical point to the origin, as in Fig. 7. The lines which pass through the data points there are just splines drawn to aid the eye in following the trajectories. Note that the curves tend to asymptote to the p -axis, suggesting that p falls off more slowly than $1/N$. This suggestion is corroborated by more detailed analysis of the scaling behavior of these trajectories, as will be discussed in [14].

⁶Notice that the error bars are shown rotated in the legend. This will be the case for all subsequent legends as well.

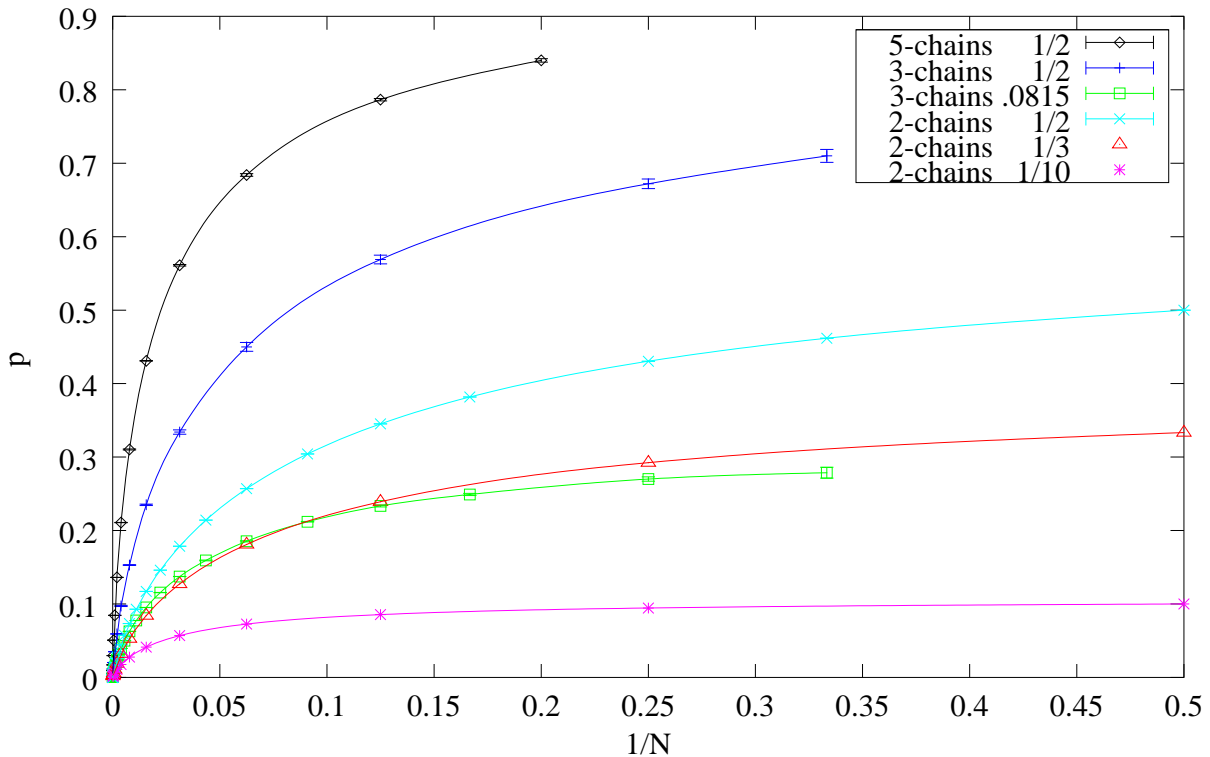


Figure 7: Six trajectories approaching the critical point at $p = 0$, $N = \infty$

6.3 Flow of the coarse-grained theory along a trajectory

We come finally to a direct test of whether the coarse-grained theory converges to a limit as $N \rightarrow \infty$. Independently of scaling or any other indicator, this is by definition the criterion for a continuum limit to exist. We have examined this question by means of simulations conducted for five of the six trajectories mentioned above. In each simulation we proceeded as follows. For each chosen N , we experimentally found a p sufficiently close to the desired trajectory. Having determined p , we then generated a large number of causet by the percolation algorithm described in Section 2. (The number generated varied from 64 to 40,000.) For each such random causet, we computed the abundances of the different m -element (sub)causet under consideration (2-chain, 3-chain, 3-antichain, etc), and we combined the results to obtain the mean abundances we have plotted here, together with their standard errors. (The errors shown do not include any contribution from the slight inaccuracy in the value of p used. Except for the 3- and 5-chain trajectories these errors are negligibly small.)

To compute the abundances of the 2-, 3-, and 4-orders for a given causet, we randomly sampled its four-element subcauset, counting the number of times each of the sixteen possible 4-orders arose, and dividing each of these counts by the number of samples taken to get the corresponding abundance. As an aid in identifying to which 4-order a sampled subcauset belonged we used the following invariant, which distinguishes all of the sixteen 4-orders, save two pairs.

$$I(S) = \prod_{x \in S} (2 + |\text{past}(x)|)$$

Here, $\text{past}(x) = \{y \in S | y \prec x\}$ is the exclusive past of the element x and $|\text{past}(x)|$ is its cardinality. Thus, we associate to each element of the causet, a number which is two more than the cardinality of its exclusive past, and we form the product of these numbers (four, in this case) to get our invariant. (For example, this invariant is 90 for the “diamond” poset, $\begin{matrix} & & \blacktriangleright & \\ & \blacktriangle & & \\ \blacktriangle & & & \\ \blacktriangle & & & \end{matrix}$.)

The number of samples taken from an N element causet was chosen to be $\sqrt{2\binom{N}{4}}$, on the grounds that the probability to get the same four element subset twice becomes appreciable with more than this many samples. Numerical tests confirmed that this rule of thumb tends to minimize the sampling error, as seen in Figure 8.

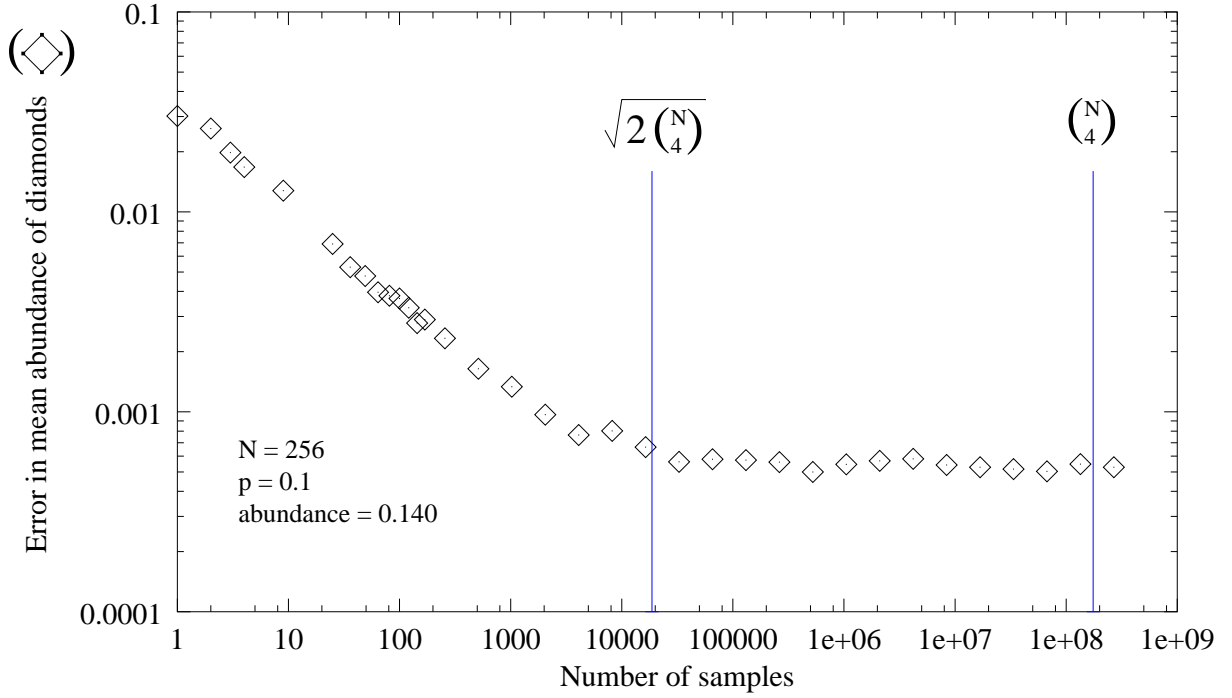


Figure 8: Reduction of error in estimated diamond abundance with increasing number of samples

Once one has the abundances of all the 4-orders, the abundances of the smaller causet can be found by further coarse graining. By explicitly carrying out this coarse graining, one easily deduces the following relationships:

$$\begin{aligned}
f_3(\mathfrak{I}) &= f_4(\mathfrak{I}) + \frac{1}{2} (f_4(\mathfrak{I}\mathfrak{I}) + f_4(\mathfrak{I}\mathfrak{I})) + \frac{1}{4}f_4(\mathfrak{I}\mathfrak{I}) + \frac{1}{4} (f_4(\mathfrak{I}\mathfrak{I}) + f_4(\mathfrak{I}\mathfrak{I})) + \frac{1}{2}f_4(\mathfrak{I}\mathfrak{I}) \\
f_3(\mathfrak{V}) &= \frac{1}{2}f_4(\mathfrak{I}\mathfrak{I}) + \frac{1}{2}f_4(\mathfrak{I}\mathfrak{I}) + \frac{1}{4}f_4(\mathfrak{I}\mathfrak{I}) + \frac{3}{4}f_4(\mathfrak{V}) + \frac{1}{4}f_4(\mathfrak{V}\mathfrak{I}) + \frac{1}{4}f_4(\mathfrak{I}\mathfrak{I}) + \frac{1}{2}f_4(\mathfrak{I}\mathfrak{I}) \\
f_3(\mathfrak{I}\mathfrak{I}) &= \frac{3}{4}f_4(\mathfrak{I}\mathfrak{I}) + \frac{1}{4} (f_4(\mathfrak{I}\mathfrak{I}) + f_4(\mathfrak{I}\mathfrak{I})) + \frac{1}{2} (f_4(\mathfrak{V}\mathfrak{I}) + f_4(\mathfrak{I}\mathfrak{I})) + f_4(\mathfrak{I}\mathfrak{I}) + \frac{1}{2}f_4(\mathfrak{I}\mathfrak{I}) + \frac{1}{2}f_4(\mathfrak{I}\mathfrak{I}) \\
f_3(\mathfrak{I}\mathfrak{I}) &= \frac{1}{2}f_4(\mathfrak{I}\mathfrak{I}) + \frac{1}{2}f_4(\mathfrak{I}\mathfrak{I}) + \frac{1}{4}f_4(\mathfrak{I}\mathfrak{I}) + \frac{3}{4}f_4(\mathfrak{I}\mathfrak{I}) + \frac{1}{4}f_4(\mathfrak{I}\mathfrak{I}) + \frac{1}{4}f_4(\mathfrak{I}\mathfrak{I}) + \frac{1}{2}f_4(\mathfrak{I}\mathfrak{I}) \\
f_3(\mathfrak{I}\mathfrak{I}) &= \frac{1}{4} (f_4(\mathfrak{V}) + f_4(\mathfrak{I}\mathfrak{I})) + \frac{1}{4} (f_4(\mathfrak{V}\mathfrak{I}) + f_4(\mathfrak{I}\mathfrak{I})) + \frac{1}{2}f_4(\mathfrak{I}\mathfrak{I}) + f_4(\mathfrak{I}\mathfrak{I}) \\
f_2(\mathfrak{I}) &= f_3(\mathfrak{I}) + \frac{2}{3} (f_3(\mathfrak{V}) + f_3(\mathfrak{I}\mathfrak{I})) + \frac{1}{3}f_3(\mathfrak{I}\mathfrak{I}) \\
f_2(\mathfrak{I}\mathfrak{I}) &= 1 - f_2(\mathfrak{I})
\end{aligned}$$

In the first six equations, the coefficient before each term on the right is the fraction of coarse-grainings of that causet which yield the causet on the left.

In Figures 9, 10, and 11, we exhibit how the coarse-grained probabilities of all possible 2, 3, and 4 element causet vary as we follow the trajectory along which the coarse-grained 2-chain probability $f_2(\mathfrak{I}) = r$ is held at 1/2. By design, the coarse-grained probability for the 2-chain remains flat at 50%,

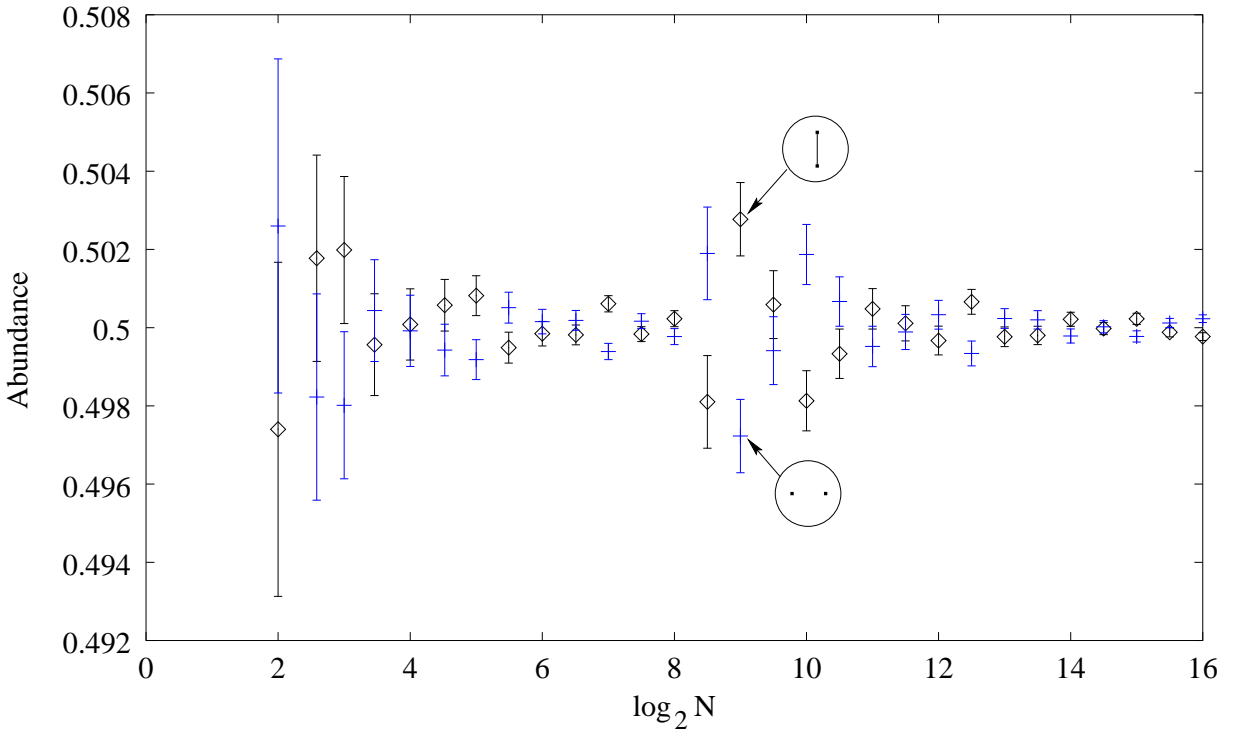


Figure 9: Flow of the coarse-grained probabilities f_m for $m = 2$. The 2-chain probability is held at $1/2$.

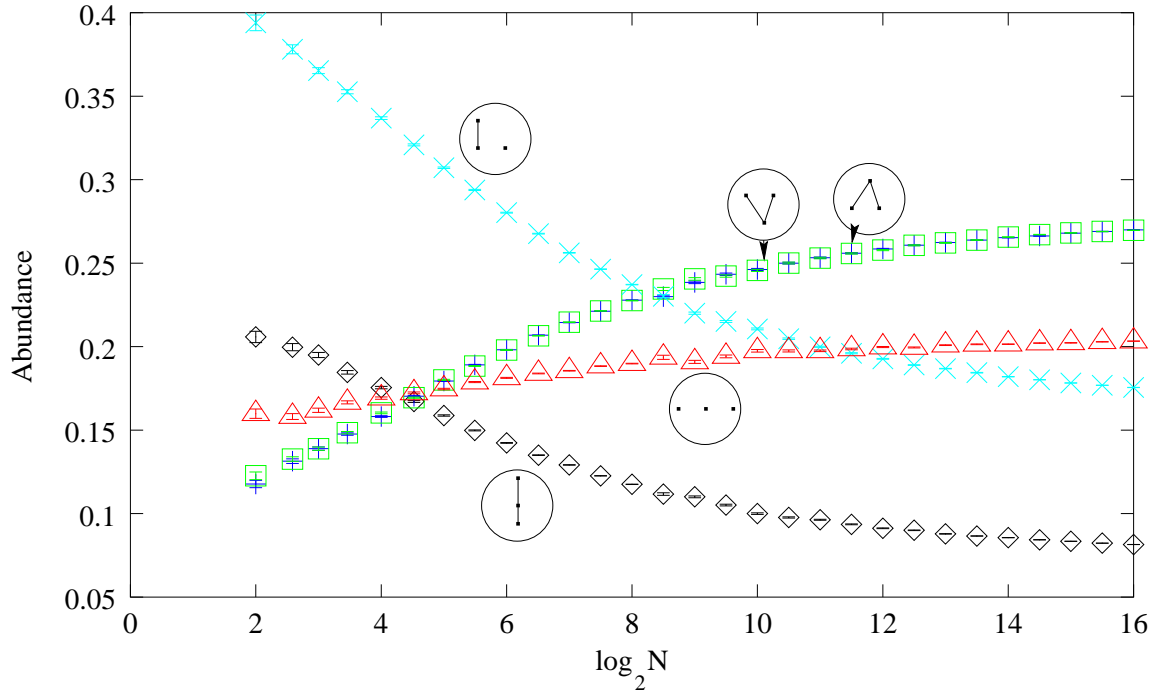


Figure 10: Flow of the coarse-grained probabilities f_m for $m = 3$. The 2-chain probability is held at $1/2$.

from the data that monotonicity will be maintained. From this, it would follow that the probabilities for ∇ and \blacktriangledown (which must be equal by time-reversal symmetry) and the other rising probabilities, \blacktriangleright , $\bullet\bullet\bullet$, and \blacktriangleright , all approach nontrivial limits. The coarse-graining to 4 elements, therefore, would also admit a continuum limit with a minimum of 4 out of the 11 independent probabilities being nontrivial.

To the extent that the $m = 2$ and $m = 3$ cases are indicative, then, it is reasonable to conclude that percolation dynamics admits a continuum limit which is non-trivial at all “scales” m .

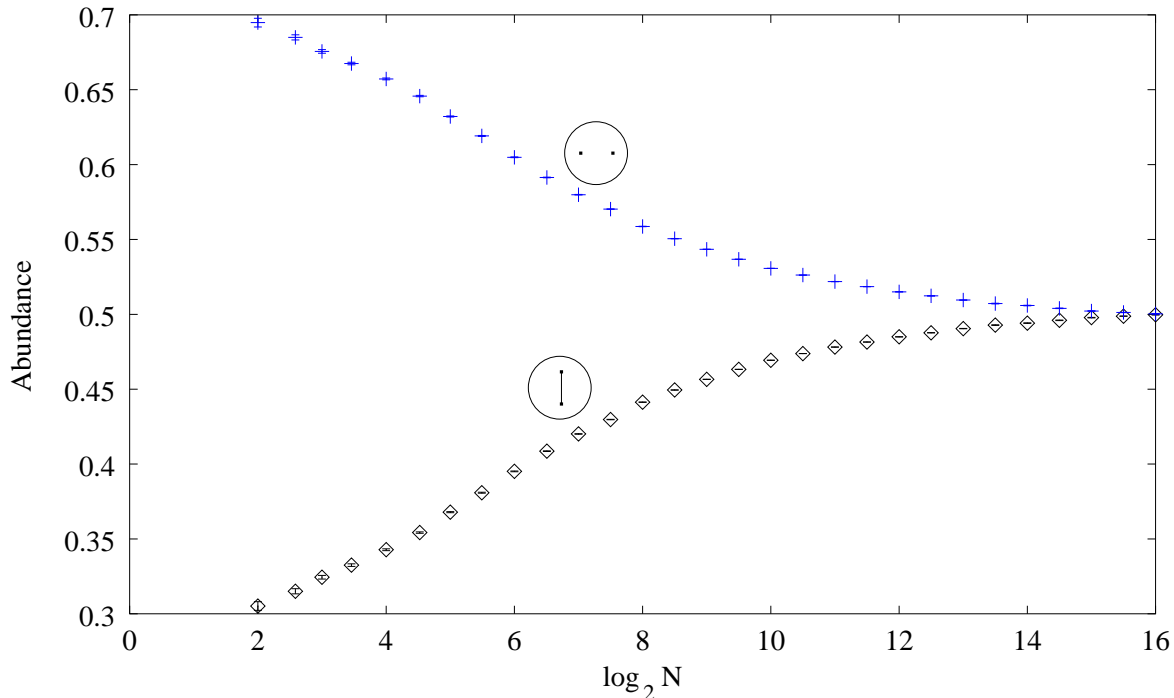


Figure 12: Flow of the coarse-grained probabilities f_m for $m = 2$. The 3-chain probability is held at 0.0814837.

The question suggests itself, whether the flow of the coarse-grained probabilities would differ qualitatively if we held fixed some abundance other than that of the 2-chain. In Figures 12, 13, and 14, we display results obtained by fixing the 3-chain abundance (its value having been chosen to make the abundance of 2-chains be $1/2$ when $N = 2^{16}$). Notice in Figure 12 that the abundance of 2-chains varies considerably along this trajectory, whilst that of the 3-chain (in figure 13) of course remains constant. Once again, the figures suggest strongly that the trajectory is approaching a continuum limit, with nontrivial values for the coarse-grained probabilities of at least the 3-chain, the “V” and the “ Λ ” (and in consequence, nontrivial values for the 2-chain and 2-antichain as well).

All the trajectories discussed so far produce causet with an ordering fraction r close to $1/2$ for large N . As mentioned earlier, $r = 1/2$ corresponds to a Myrheim-Meyer dimension of two. Figures 15 and 16 show the results of a simulation along the “four dimensional” trajectory defined by $r = 1/10$. (The value $r = 1/10$ corresponds to a Myrheim-Meyer dimension of 4.) Here the appearance of the flow is much less elaborate, with the curves arrayed simply in order of increasing ordering fraction, $\bullet\bullet\bullet$ and $\bullet\bullet\bullet\bullet$ being at the top and \updownarrow and (imperceptibly) \updownarrow at the bottom. As before, all the curves are monotone as far as can be seen. Aside from the intrinsic interest of the case $d = 4$, these results indicate that our conclusions drawn for d near 2 will hold good for all larger d as well.

Figure 17 displays the flow of the coarse-grained probabilities from a simulation in the opposite situation where the ordering fraction is much greater than $1/2$ (the Myrheim-Meyer dimension is down near 1.) Shown are the results of coarse-graining to three element causet along the trajectory which

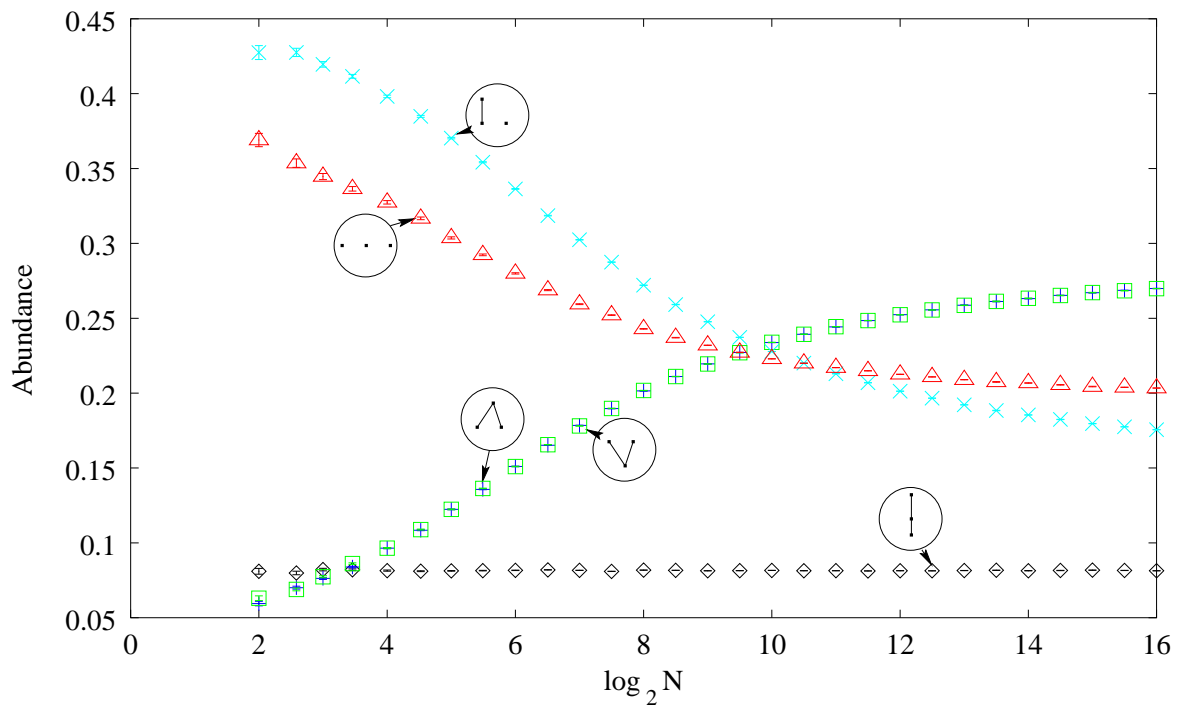


Figure 13: Flow of the coarse-grained probabilities f_m for $m = 3$. The 3-chain probability is held at 0.0814837.

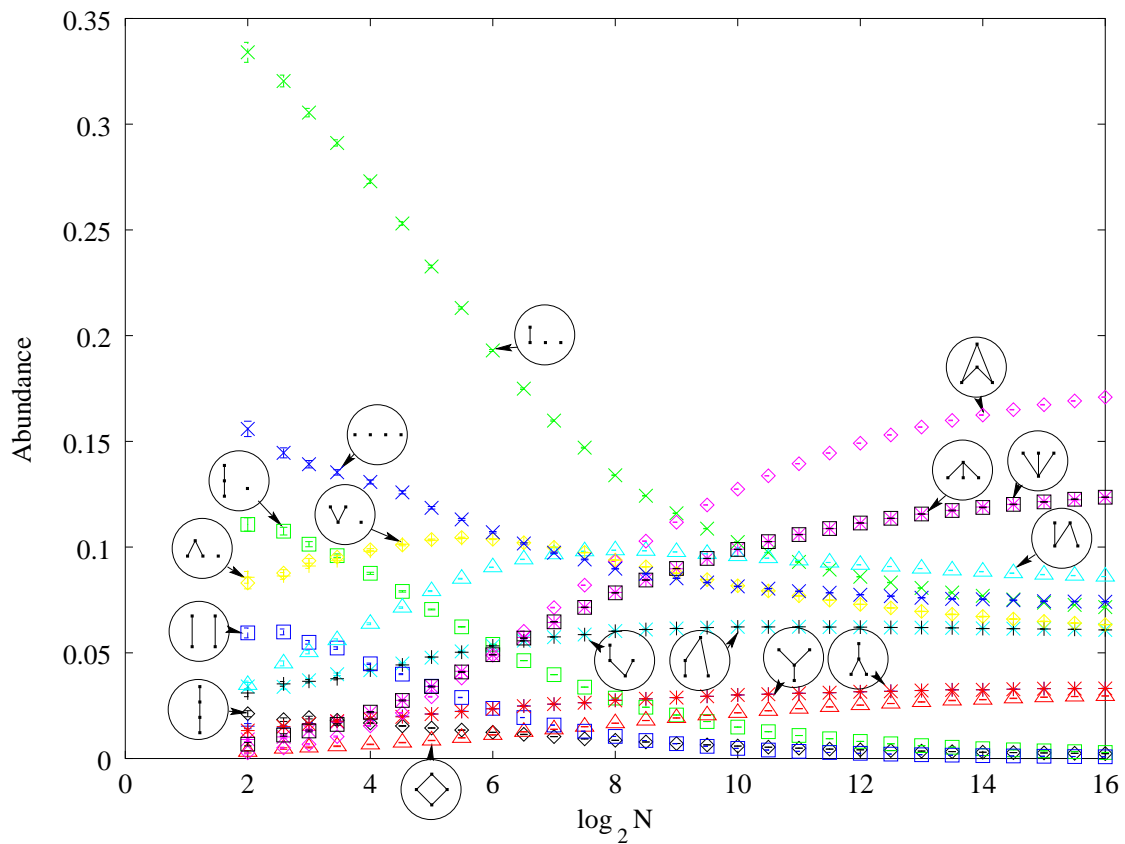


Figure 14: Flow of the coarse-grained probabilities f_m for $m = 4$. The 3-chain probability is held at 0.0814837.

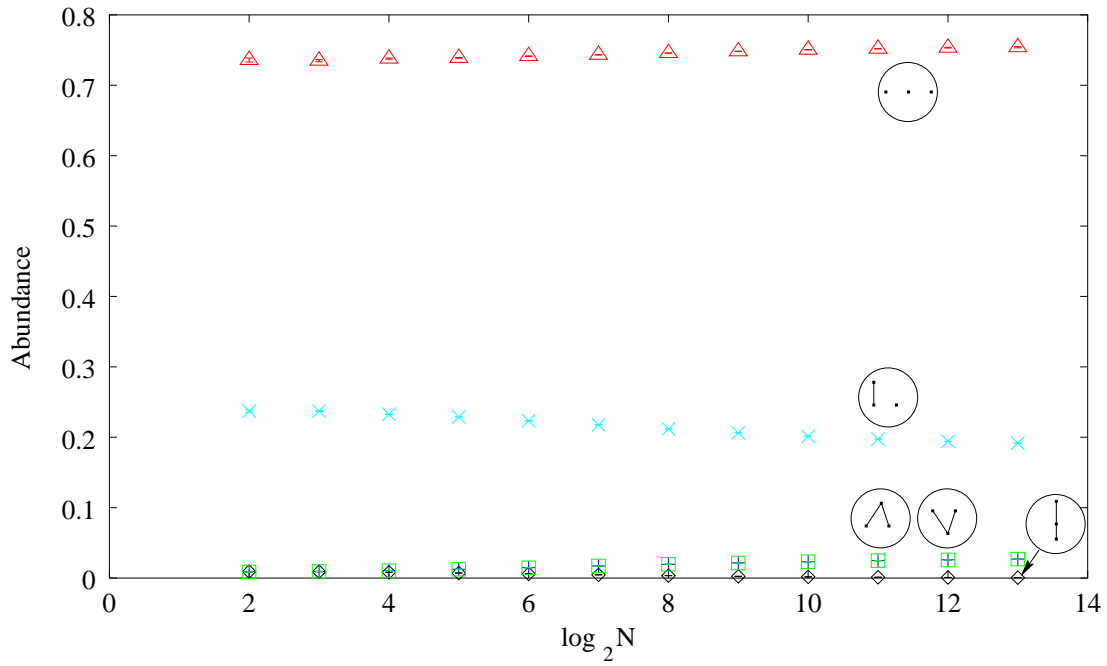


Figure 15: Flow of the coarse-grained probabilities f_m for $m = 3$. The 2-chain probability is held at $1/10$.

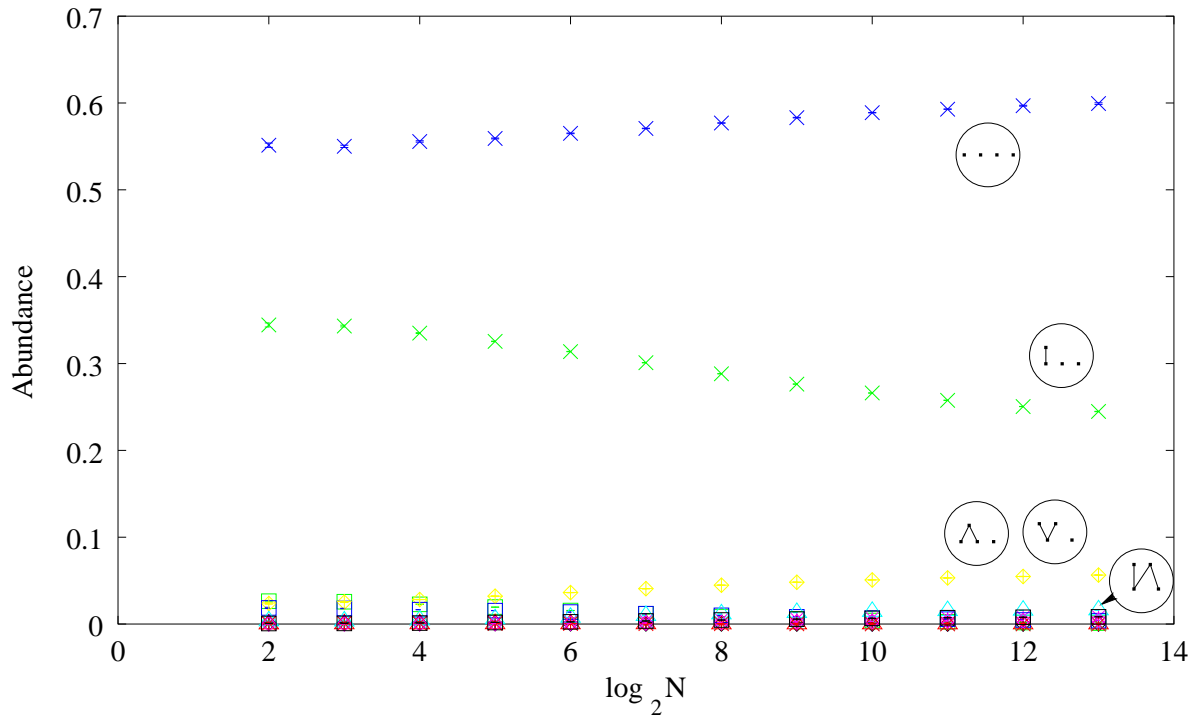


Figure 16: Flow of the coarse-grained probabilities f_m for $m = 4$. The 2-chain probability is held at $1/10$. Only those curves lying high enough to be seen distinctly have been labeled.

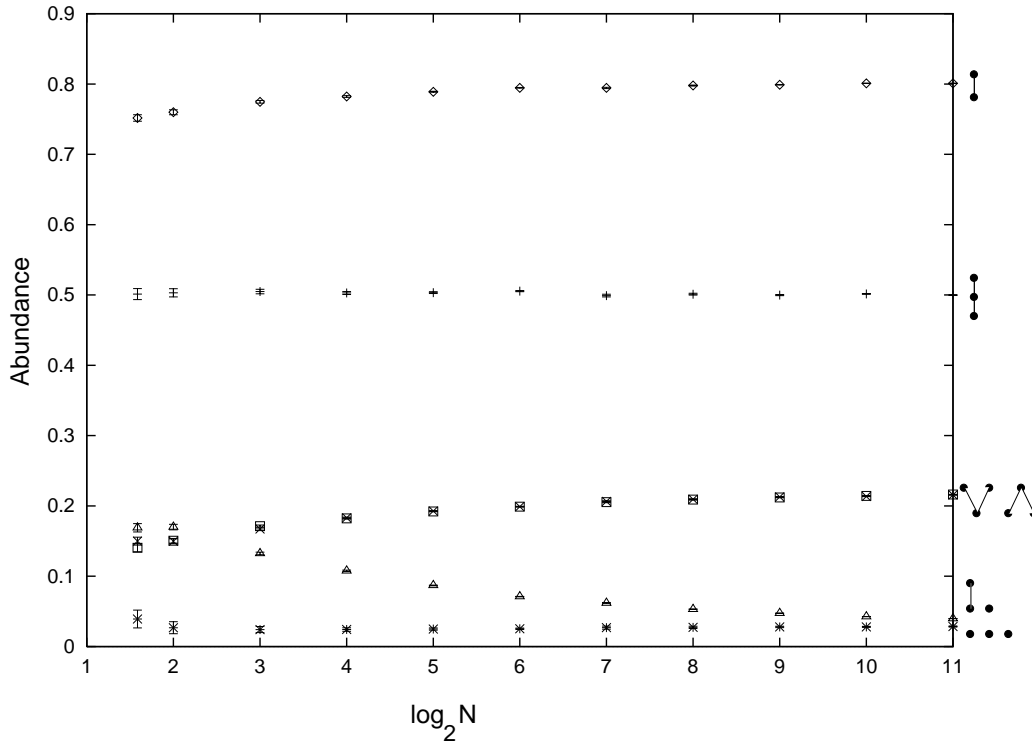


Figure 17: Flow of the coarse-grained probabilities f_m for $m = 3$. The 3-chain probability is held at $1/2$.

holds the 3-chain probability to $1/2$. Also shown is the 2-chain probability. The behavior is similar to that of Figure 15, except that here the coarse-grained probability rises with the ordering fraction instead of falling. This occurs because constraining $f_3(\mathfrak{I})$ to be $1/2$ generates rather chain-like causets whose Myrheim-Meyer dimension is in the neighborhood of 1.34, as follows from the approximate limiting value $f_2(\mathfrak{I}) \approx 0.8$. The slow, monotonic, variation of the probabilities at large N , along with the appearance of convergence to non-zero values in each case, suggests the presence of a nontrivial continuum limit for r near unity as well.

Figures 18 and 19 present the results of a final set of simulations, the only ones we have carried out which examined the abundances of causets containing more than four elements. In these simulations, the mean 5-chain abundance $f_5(\text{5-chain})$ was held at $1/2$, producing causets that were even more chain-like than before (Myrheim-Meyer dimension ≈ 1.1). Figure 18 tracks the resulting abundances of all k -chains for k between 2 and 7, inclusive. (We limited ourselves to chains, because their abundances are relatively easy to determine computationally.) As in Figure 17, all the coarse-grained probabilities appear to be tending monotonically to limits at large N . In fact, they look amazingly constant over the whole range of N , from 5 to 2^{15} . One may also observe that, as one might expect, the coarse-grained probability of a chain decreases markedly with its length (and almost linearly over the range examined!). It appears also that the k -chain curves for $k \neq 5$ are “expanding away” from the 5-chain curve, but only very slightly. Figure 19 tracks the abundances of all the four-element causets. It is qualitatively similar to Figures 15–17, with very flat probability curves, and here with a strong preference for causets having many relations over those having few.

Comparing Figures 19 and 16 with Figures 14 and 11, one can observe that trajectories which generate causets that are rather chain-like or antichain-like seem to produce distributions which converge more rapidly than those along which the ordering fraction takes values close to $1/2$.

In the way of further simulations, it would be extremely interesting to look for continuum limits

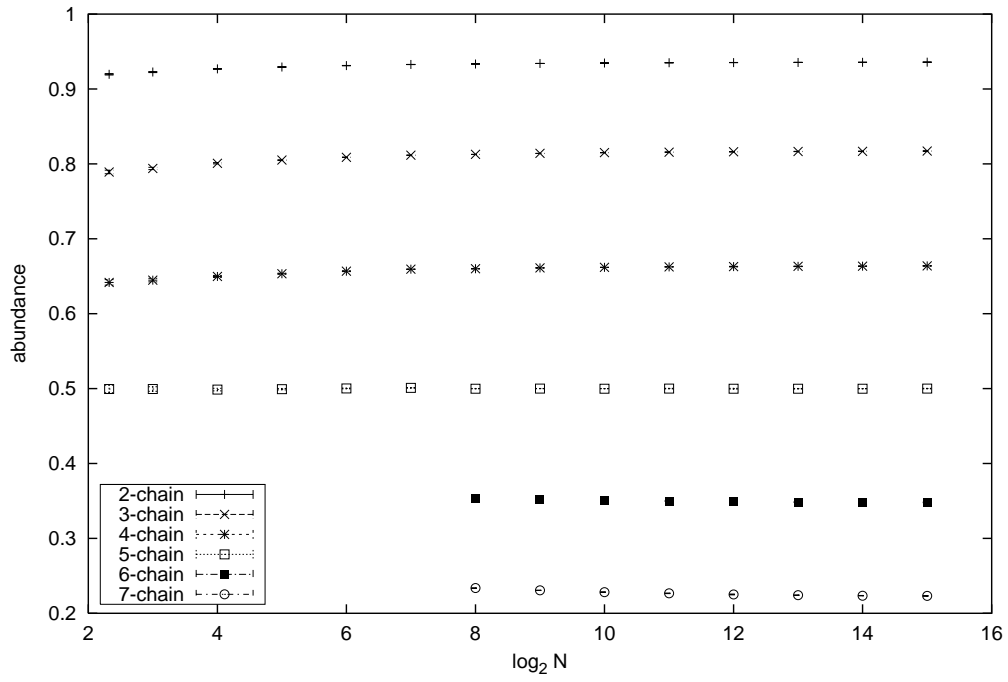


Figure 18: Flow of the coarse-grained probabilities $f_m(m\text{-chain})$ for $m = 2$ to 7. The 5-chain probability is held at $1/2$.

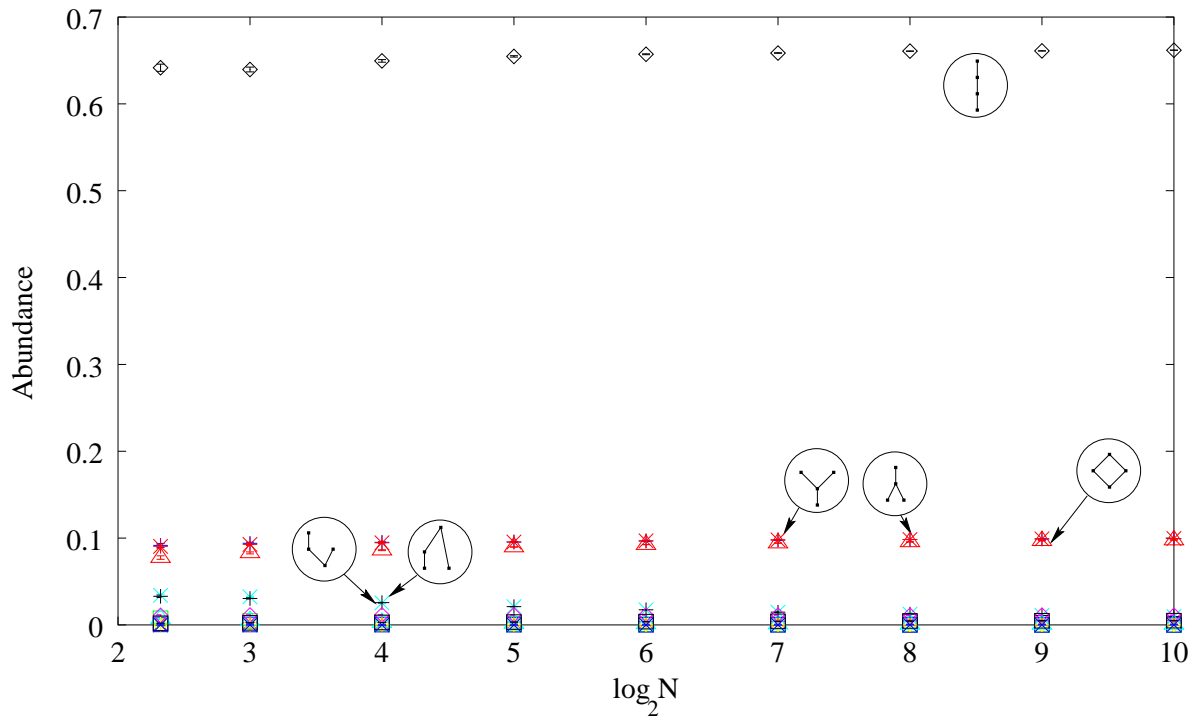


Figure 19: Flow of the coarse-grained probabilities f_m for $m = 4$. The 5-chain probability is held at $1/2$.

of some of the more general dynamical laws discussed in §4.5 of Reference [1]. In doing so, however, one would no longer have available (as one does have for transitive percolation) a very fast (yet easily coded) algorithm that generates causets randomly in accord with the underlying dynamical law. Since the sequential growth dynamics of [1] is produced by a stochastic process defined recursively on the causal set, it is easily mimicked algorithmically; but the most obvious algorithms that do so are too slow to generate efficiently causets of the size we have discussed in this paper. Hence, one would either have to devise better algorithms for generating causets “one off”, or one would have to use an entirely different method to obtain the mean abundances, like Monte Carlo simulation of the random causet.

7 Concluding Comments

Transitive percolation is a discrete dynamical theory characterized by a single parameter p lying between 0 and 1. Regarded as a stochastic process, it describes the steady growth of a causal set by the continual birth or “accretion” of new elements. If we limit ourselves to that portion of the causet comprising the elements born between step N_0 and step N_1 of the stochastic process, we obtain a model of random posets containing $N = N_1 - N_0$ elements. This is the model we have studied in this paper.

Because the underlying process is homogeneous, this model does not depend on N_0 or N_1 separately, but only on their difference. It is therefore characterized by just two parameters p and N . One should be aware that this truncation to a finite model is not consistent with discrete general covariance, because it is the subset of elements with certain *labels* that has been selected out of the larger causet, rather than a subset characterized by any directly physical condition. Thus, we have introduced an “element of gauge” and we hope that we are justified in having neglected it. That is, we hope that the random causets produced by the model we have actually studied are representative of the type of suborder that one would obtain by percolating a much larger (eventually infinite) causet and then using a label-invariant criterion to select a subset of N elements.

Leaving this question aside for now, let us imagine that our model represents an interval (say) in a causet C underlying some macroscopic spacetime manifold. With this image in mind, it is natural to interpret a continuum limit as one in which $N \rightarrow \infty$ while the coarse-grained features of the interval in question remain constant. We have made this notion precise by defining coarse-graining as random selection of a suborder whose cardinality m measures the “coarseness” of our approximation. A continuum limit then is defined to be one in which N tends to ∞ such that, for each finite m , the induced probability distribution f_m on the set of m -element posets converges to a definite limit, the physical meaning being that the dynamics at the corresponding length-scale is well defined. Now, how could our model *fail* to admit such a limit?

In a field-theoretic setting, failure of a continuum limit to exist typically means that the coarse-grained theory loses parameters as the cutoff length goes to zero. For example, $\lambda\phi^4$ scalar field theory in 4 dimensions depends on two parameters, the mass μ and the coupling constant λ . In the continuum limit, λ is lost, although one can arrange for μ to survive. (At least this is what most workers believe occurs.) Strictly speaking, one should not say that a continuum limit fails to exist altogether, but only that the limiting theory is poorer in coupling constants than it was before the limit was taken. Now in our case, we have only one parameter to start with, and we have seen that it does survive as $N \rightarrow \infty$ since we can, for example, choose freely the $m = 2$ coarse-grained probability distribution f_2 . Hence, we need not fear such a loss of parameters in our case.

What about the opposite possibility? Could the coarse-grained theory *gain* parameters in the $N \rightarrow \infty$ limit, as might occur if the distributions f_m were sensitive to the fine details of the trajectory along which N and p approached the “critical point” $p = 0, N = \infty$?⁷ Our simulations showed no sign of such

⁷Such an increase of the parameter set through a limiting process seems logically possible, although we know of no example of it from field theory or statistical mechanics, unless one counts the extra global parameters that come in with

sensitivity, although we did not look for it specifically. (Compare, for example, Figure 10 with Figure 13 and 11 with 14.)

A third way the continuum limit could fail might perhaps be viewed as an extreme form of the second. It might happen that, no matter how one chose the trajectory $p = p(N)$, some of the coarse-grained probabilities $f_m(\xi)$ oscillated indefinitely as $N \rightarrow \infty$, without ever settling down to fixed values. Our simulations leave little room for this kind of breakdown, since they manifest the exact opposite kind of behavior, namely monotone variation of all the coarse-grained probabilities we “measured”.

Finally, a continuum limit could exist in the technical sense, but it still could be effectively trivial (once again reminiscent of the $\lambda\phi^4$ case — if you care to regard a free field theory as trivial.) Here triviality would mean that all — or almost all — of the coarse-grained probabilities $f_m(\xi)$ converged either to 0 or to 1. Plainly, we can avoid this for at least some of the $f_m(\xi)$. For example, we could choose an m and hold either $f_m(m\text{-chain})$ or $f_m(m\text{-antichain})$ fixed at any desired value. (Proof: as $p \rightarrow 1$, $f_m(m\text{-chain}) \rightarrow 1$ and $f_m(m\text{-antichain}) \rightarrow 0$; as $p \rightarrow 0$, the opposite occurs.) However, in principle, it could still happen that all the other f_m besides these two went to 0 in the limit. (Clearly, they could not go to 1, the other trivial value.) Once again, our simulations show the opposite behavior. For example, we saw that $f_3(\mathbf{V})$ increased monotonically along the trajectory of Figure 10.

Moreover, even without reference to the simulations, we can make this hypothetical “chain-antichain degeneracy” appear very implausible by considering a “typical” causet C generated by percolation for $N \gg 1$ with p on the trajectory that, for some chosen m , holds $f_m(m\text{-chain})$ fixed at a value a strictly between 0 and 1. Then our degeneracy would insist that $f_m(m\text{-antichain}) = 1 - a$ and $f_m(\chi) = 0$ for all other χ . But this would mean that, in a manner of speaking, “every” coarse-graining of C to m elements would be either a chain or an antichain. In particular the causet $\mathbf{!}_\bullet$ could not occur as a subcauset of C ; whence, since $\mathbf{!}_\bullet$ is a subcauset of every m -element causet except the chain and the antichain, C itself would have to be either an antichain or a chain. But it is absurd that percolation for any parameter value p other than 0 and 1 would produce a “bimodal” distribution such that C would have to be either a chain or an antichain, but nothing in between. (It seems likely that similar arguments could be devised against the possibility of similar, but slightly less trivial trivial continuum limits, for example a limit in which $f_m(\chi)$ would vanish unless χ were a disjoint union of chains and antichains.)

Putting all this together, we have persuasive evidence that the percolation model does admit a continuum limit, with the limiting model being nontrivial and described by a single “renormalized” parameter or “coupling constant”. Furthermore, the associated scaling behavior one might anticipate in such a case is also present, as we will discuss further in [14].

But is the word “continuum” here just a metaphor, or can it be taken more literally? This depends, of course, on the extent to which the causets yielded by percolation dynamics resemble genuine spacetimes. Based on the meager evidence available at the present time, we can only answer “it is possible”. On one hand, we know [1] that any spacetime produced by percolation would have to be homogeneous, like de Sitter space or Minkowski space. We also know, from simulations in progress, that two very different dimension estimators seem to agree on percolated causets, which one might not expect, were there no actual dimensions for them to be estimating. Certain other indicators tend to behave poorly, on the other hand, but they are just the ones that are *not* invariant under coarse-graining (they are not “RG invariants”), so their poor behavior is consistent with the expectation that the causal set will not be manifold-like at the smallest scales (“foam”), but only after some degree of coarse-graining.

Finally, there is the ubiquitous issue of “fine tuning” or “large numbers”. In any continuum situation, a large number is being manifested (an actual infinity in the case of a true continuum) and one may wonder where it came from. In our case, the large numbers were p^{-1} and N . For N , there is no mystery: unless the birth process ceases, N is guaranteed to grow as large as desired. But why should p be so small? Here, perhaps, we can appeal to the preliminary results of Dou mentioned in the introduction. If

“spontaneous symmetry breaking”.

— cosmologically considered — the causet that is our universe has cycled through one or more phases of expansion and recollapse, then its dynamics will have been filtered through a kind of “temporal coarse-graining” or “RG transformation” that tends to drive it toward transitive percolation. But what we didn’t mention earlier was that the parameter p of this effective dynamics scales like $N_0^{-1/2}$, where N_0 is the number of elements of the causet preceding the most recent “bounce”. Since this is sure to be an enormous number if one waits long enough, p is sure to become arbitrarily small if sufficiently many cycles occur. The reason for the near flatness of spacetime — or if you like for the large diameter of the contemporary universe — would then be just that the underlying causal set is very old — old enough to have accumulated, let us say, 10^{480} elements in earlier cycles of expansion, contraction and re-expansion.

It is a pleasure to thank Alan Daughton, Chris Stephens, Henri Waelbroeck and Denjoe ÓConnor for extensive discussions on the subject of this paper. The research reported here was supported in part by NSF grants PHY-9600620 and INT-9908763 and by a grant from the Office of Research and Computing of Syracuse University.

References

- [1] D. P. Rideout and R. D. Sorkin, “Classical sequential growth dynamics for causal sets,” *Physical Review D*, vol. 61, p. 024002, Jan. 2000. <e-print archive: gr-qc/9904062>.
- [2] Graham Brightwell “Models of Random Partial Orders” in *Surveys in Combinatorics, 1993*, London Math. Soc. Lecture Notes Series **187**:53–83, ed. Keith Walker (Cambridge Univ. Press 1993)
 Béla Bollobás and Graham Brightwell, “The structure of random graph orders”, *SIAM J. Discrete Math.***10**: 318–335 (1997)
 Béla Bollobás and Graham Brightwell, “The dimension of random graph orders”, in *The Mathematics of Paul Erdős II*, R.L. Graham and J. Nešetřil, eds. (Springer-Verlag, 1996), pp. 51–69
 Béla Bollobás and Graham Brightwell, “The width of random graph orders”, *Math. Scientist* **20**: 69–90 (1995)
 B. Pittel and R. Tungal, “A Phase Transition Phenomenon in a Random Directed Acyclic Graph”, (Ohio State preprint, ?1998)
 D. Crippa, K. Simon and P. Trunz, “Markov Processes Involving q -Stirling Numbers”, *Combinatorics, Probability and Computing* **6**: 165–178 (1997)
 Klaus Simon, Davide Crippa and Fabian Collenberg, “On the Distribution of the Transitive Closure in a Random Acyclic Digraph”, *Lecture Notes in Computer Science* **726**: 345–356 (1993)
 K. Simon, “Improved Algorithm for Transitive Closure on Acyclic Digraphs”, *Theoretical Computer Science* **58** (1988).
- [3] N. Alon, B. Bollobás, G. Brightwell, and S. Janson, “Linear extensions of a random partial order,” *Ann. Applied Prob.*, vol. 4, pp. 108–123, 1994.
- [4] L. Bombelli, *Spacetime as a Causal Set*. PhD thesis, Syracuse University, December 1987.
- [5] L. Bombelli, J. Lee, D. Meyer, and R. D. Sorkin, “Space-time as a causal set,” *Physical Review Letters*, vol. 59, pp. 521–524, 1987.
- [6] D. Reid, “Introduction to causal sets: an alternative view of spacetime structure.” <e-print archive: gr-qc/9909075>, 1999.
- [7] R. D. Sorkin, “Spacetime and causal sets,” in *Relativity and Gravitation: Classical and Quantum* (J. C. D’Olivo, E. Nahmad-Achar, M. Rosenbaum, M. Ryan, L. Urrutia, and F. Zertuche, eds.),

(Singapore), pp. 150–173, World Scientific, December 1991. (Proceedings of the *SILARG VII Conference*, held Cocoyoc, Mexico, December, 1990).

- [8] D. Dou, *Causal Sets, a Possible Interpretation for the Black Hole Entropy, and Related Topics*. PhD thesis, SISSA, Trieste, 1999.
- [9] B. Bollobás and G. Brightwell, “Graphs whose every transitive orientation contains almost every relation,” *Israel Journal of Mathematics*, vol. 59, no. 1, pp. 112–128, 1987.
- [10] C. M. Newman and L. S. Schulman, “One-dimensional $1/|j - i|^s$ percolation models: The existence of a transition for $s \leq 2$,” *Commun. Math. Phys.*, vol. 104, no. 4, pp. 547–571, 1986.
- [11] J. Myrheim, “Statistical geometry,” CERN preprint TH-2538 (1978).
- [12] A. Daughton, *The Recovery of Locality for Causal Sets and Related Topics*. PhD thesis, Syracuse University, 1993.
- [13] A. Daughton, R. D. Sorkin, and C. Stephens, “Percolation and causal sets: A toy model of quantum gravity,” (in preparation).
- [14] D. P. Rideout and R. D. Sorkin, “Evidence for scaling in the continuum limit of percolated causal sets,” (in preparation).
- [15] D. A. Meyer, *The Dimension of Causal Sets*. PhD thesis, Massachusetts Institute of Technology, 1988.